THE EFFECT OF POSS FILLERS IN NON-ISOCYANATE POLYURETHANE HYBRID RESINS

*Carlee M. MacInnis, Georges R. Younes, and Milan Marić**

C. M. MacInnis, Dr. G. R. Younes, Prof. M. Marić
Department of Chemical Engineering
McGill University
Montreal, Quebec H3A 0C5, Canada
E-mail: milan.maric@mcgill.ca

ABSTRACT

Polyhedral oligomeric silsesquioxane (POSS) are added to poly(hydroxyurethanes) PHU prepolymers to create hybrid PHUs (HPHU)s with enhanced mechanical and thermal properties. These hybrid materials were then further functionalized with 3-Isocyanatopropyl(trimethoxy) silane (IPTMS) via the pendant hydroxyl bonds within the backbone of the polymers to obtain a final cured film comparable to conventional polyurethanes (PU), using less isocyanate-functional material. The incorporation of POSS into PHU prepolymers to obtain HPHUs was supported by GPC, FTIR and NMR analysis. Furthermore, the thermal degradation of the HPHUs was significantly improved with increasing POSS concentration compared to their PHU counterparts as the degradation temperatures at 50 % weight loss increased from 263 °C for the PHU to 341 °C for the HPHU. Gel content tests in THF, water, and toluene were performed and gel contents of 87-99 % in THF were observed for the cured films. Water swelling, and contact angle tests confirmed that the POSS-modified films exhibited hydrophobic behaviour. Finally, mechanical properties of the cured films were investigated. The Young's modulus and tensile strength were improved with increasing POSS concentration (from 2.0 to 3.1 MPa and from 0.82 to 1.32 MPa, respectively) and elongations at break up to 41.6 % were observed. When compared to a conventional PU sealant, the HPHU achieved a tensile strength that was two-fold greater and a comparable elongation at break (increasing from 24.8% to as high as 41.6%).

1. INTRODUCTION

Since their discovery in the 1930's by Bayer *et al.*, the use of polyurethanes (PUs) has expanded greatly and they are now one of the most versatile classes of polymers.[1] In 2020, the worldwide production of all plastics was 367 million tonnes and PUs made up 7.8 %, making them the 7th most highly produced type of polymer used in the production of plastics.[2] Most PUs are typically synthesized via a polyaddition reaction of diols (polyols) and diisocyanates in the presence of tertiary amines as a catalyst.[3] The downside to this reaction, however, arises from the synthesis of the diisocyanates, which involves the use of lethal phosgene gas. Therefore, finding alternative routes to produce polyurethanes without the use of isocyanates is increasingly important from an environmental standpoint as the global demand for polyurethanes continues to rise.

Through using non-toxic and renewable resources, researchers have been able to develop non-isocyanate polyurethanes (NIPU) recently. Indeed, these NIPUs have even shown improved mechanical properties, thermal stability, chemical resistance, and lower permeability than conventional polyurethanes.[4] It is widely believed that the work of Groszos *et al.*[5] was the first to develop a method to prepare polyurethanes leading to the preparation of NIPUs.[4, 6] Among the different routes, a polyaddition reaction between a polycyclic carbonate and polyamine is the most popular as it does not require the use of phosgene or its derivatives.[7] This route creates a NIPU known as a polyhydroxyurethane (PHU). Polyamines are commercially available, thus making them an easily accessible reactant.[4] Polycyclic carbonates also are noted due to their high solvency and boiling points, as well as their low toxicity generally.[4] Additionally, polycyclic carbonates are reactive with aliphatic and aromatic amines, alcohols, thiols, and carboxylic acids,[8] making them a versatile group that can be tailored post-polymerization.

Those polyaddition reactions do have weaknesses when compared to standard isocyanate-based polyurethanes. The five-membered cyclic carbonates (CC) have low reactivity towards the polyamines as compared to the highly reactive isocyanates with polyols, giving lower polymerization rates for PHUs.[6] However, PHUs can be further modified due to the presence of the hydroxyl groups, allowing for a wide array of functionalized PHUs with tailored properties for specific applications.[4] Furthermore, there are several renewable resources that have recently been investigated to obtain CCs, which include vegetable oils[9-12] and other bio-based sources such as fatty acids, sugars, terpenes, glycerol, rosin gum, sorbitol, and cashew nut shells.[12, 13] Overall, the low toxicity of CCs and polyamines, as well as the abundance of renewable and sustainable resources that can be converted into bio-based precursors for this reaction, make it a desirable route compared to conventional PU synthesis.[6, 9]

Despite the growing interest in PHU development, there are some key challenges that hinder its ability to extend to industrial scale. Namely, the comparatively lower polymerization rates, as it can be difficult to achieve linear polymers with high molecular weights within a reasonable reaction time. Additionally, PHUs tend to lack the mechanical and chemical properties that are required for specific applications. To overcome these limitations, inorganic/organic materials can be added with PHUs to create what is known as a Hybrid PHU (HPHU). HPHUs have drawn much interest as an attractive alternative to standard PUs. These hybrid materials can combine desired properties from different materials to create a product that is less toxic (in NIPU form) with enhanced mechanical properties. Most studies have focused on three main routes for the synthesis of HPHUs, via epoxies, siloxanes, and acrylics. Studies that used epoxies in their HPHU formulation took different approaches, such as using PHU prepolymers,[14-18] carbonated epoxide monomers,[19-25] and hydroxyurethane modifiers.[26-28] Similarly, studies that focused on silicones

applied siloxane-containing monomers,[29, 30] polyhedral oligomeric silsesquioxanes (POSS),[30-35] and sol-gel methods.[36-39] Finally, acrylic based routes for HPHU synthesis employed amine terminated PHU prepolymers,[40-43] hydroxyurethane methacrylates,[44-47] and pendant cyclic carbonate functional prepolymers.[48-52] In addition to these routes, other hybrid approaches have been particularly applied with waterborne HPHUs[53-55] which have been reviewed recently.[56-58] Namely, these routes are hybrids in that the urethanes are functionalized and hybridized, for example, with monomers employing free radical polymerization methods. Overall, the above methods give promising approaches towards obtaining HPHUs that are comparable to conventional PUs. Most studies have been able to achieve, and sometimes even exceed some of the desired properties of typical PUs, but still fall short in some key areas. This study aims to provide a novel approach to develop a HPHU that addresses some of the main limitations of previously reported PHUs and HPHUs. The HPHUs in this case will be formulated using a combination of the different approaches mentioned. Specifically, a sol-gel route via the addition of POSS to linear PHU prepolymers is presented. In this step, no isocyanates or toxic chemicals were used to obtain HPHUs, however in subsequent curing reactions, an isocyanate silane agent was used to obtain a final cured film. POSS is a class of inorganic-organic hybrid compounds that have attracted much interest for many applications. For polymers specifically, POSS has been shown to significantly improve mechanical properties, thermal stability, water tolerance, fire resistance, and dielectric properties.[32]

In this work, diglycerol dicarbonate (DGC)-based PHUs were synthesized from amino-telechelic poly(propylene oxide) (Jeffamine D series) of different molecular weights to obtain a PHU prepolymer. These prepolymers were then functionalized to obtain POSS moieties as end groups to obtain a HPHU, that can be mixed with a similar PHU before curing. These HPHUs

were then further functionalized via the pendant hydroxyl bonds in the backbone of the polymer with an isocyanate silane moisture curing agent to obtain a final cured film. The curing kinetics, and mechanical and thermal properties of the cross-linked films are reported and compared to their PHU counterparts as well as a conventional PU.

2. Results and Discussion

2.1 Synthesis of Hybrid POSS PHUs

The PHU prepolymers synthesized in this work were previously optimized by Younes *et al.*[36] The characterization results via FTIR, and ^{1}H NMR for these PHU prepolymers can be found in Section 1 of the Supporting Information. The PHU prepolymers were synthesized to give CC functionality, allowing for the addition of the aminopropyl isobutyl POSS (A-POSS) on the ends of the polymer to give a telechelic HPHU resin, as shown in **Scheme 1**. Careful attention was directed towards ensuring the A-POSS was covalently bonded to the polymer and not just mixed separately, like an additive.

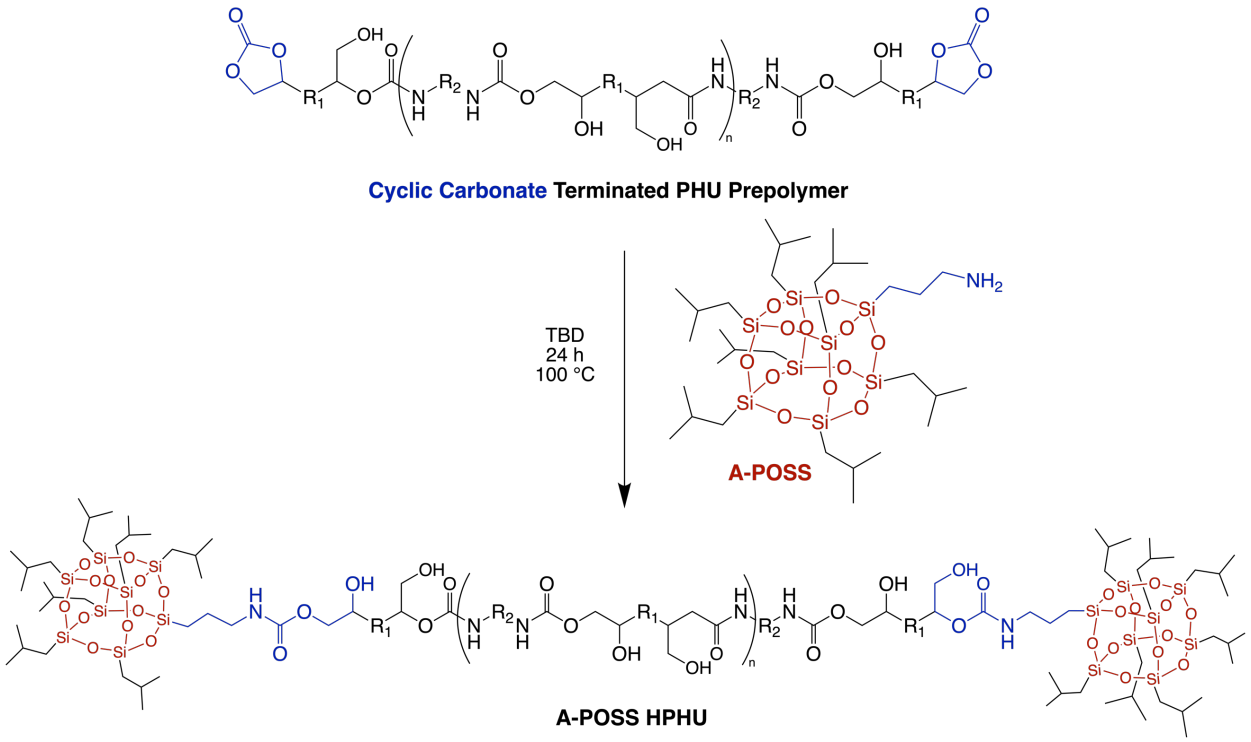

Scheme 1: Synthesis of a POSS-capped HPHU resin from a PHU prepolymer followed by capping with A-POSS. R_1 represents the chain of the cyclic dicarbonate monomer and R_2 represents the chain of the diamine monomer; the number of polymer units, n=3.

The synthesis of the A-POSS-terminated HPHU was first attempted with the CC terminated PHU prepolymer, but without the use of a catalyst, which was unsuccessful. This is attributed to

the lower reactivity of CCs to amine[8] as well as the bulky nature of POSS. Next, similar reaction conditions were used to obtain A-POSS HPHUs, but 1,5,7-triazabicyclo[4.4.0]dec-5-ene (TBD) was also added as a catalyst with the CC terminated PHU prepolymer. This method was ultimately successful, however several trials were required to determine the optimal TBD concentration as excessive catalyst caused unwanted side reactions that formed urea, which will be further discussed in the following section.

It should be noted that the last method resulted in A-POSS terminated HPHUs with Jeffamine D-2000 in the backbone (the prepolymer was based on DGC with Jeffamine D-2000) using of TBD as a catalyst. Taking the reaction conditions found from this method, this synthesis was then slightly altered to create a different set of HPHUs for comparison. Specifically, PHU prepolymers were synthesized from Jeffamine D-4000 and then further functionalized with A-POSS. Almost the same reaction conditions were used for this synthesis, however longer reaction times were required due to the longer chain diamine used. This resulted in HPHUs with longer soft segments that would alter the final mechanical properties. Overall, these two sets of HPHUs were fully investigated and characterized to show how diamine selection can affect the final properties.

2.1.1 FTIR Results

FTIR was used to track the various bonds that were forming and disappearing in the reaction between the PHU prepolymer and A-POSS. The FTIR spectra given in **Figure 1** shows the comparison of the PHU prepolymer (2K-PHU) to an unsuccessful HPHU synthesis (HPHU-A3.7) and a successful HPHU synthesis (HPHU-A3.20) along with their reaction conditions. This spectrum shows the C=O bond of the CC end groups and the urethane linkages at 1800 cm^{-1} and 1720 cm^{-1}, respectively. These were the main peaks that were investigated during FTIR analysis as the CC peaks are expected to diminish while the urethane peak increases. This occurs because

as the CC end groups of the PHU prepolymer react with the amine of the POSS, the CC groups will turn into urethane bonds, which will be reflected in the FTIR spectra. The unsuccessful HPHU synthesis (HPHU-A3.7), shows the CC peak disappears at 1800 cm^{-1}, however there is also a significant decrease in the urethane peak at 1720 cm^{-1} and a new peak from 1650 cm^{-1} to 1675 cm^{-1}. This new peak is indicative of urea formation.[59] This reaction used a TBD concentration of 2.5 mol%, which was ultimately found to be too high as it caused the formation of urea and because of this, no further characterization was done for this sample. In the successful HPHU synthesis, there is a decrease in the CC peak at 1800 cm^{-1} while the urethane peak at 1720 cm^{-1} shows a slight increase. This indicates that the CC end groups of the PHU prepolymer were reacted with the A-POSS, signifying the successful incorporation of POSS into the polymer. This was achieved by using a lower TBD concentration of 0.5 mol% at 100 °C for 24 h. These reactions used Jeffamine D-2000 as the amine and the corresponding FTIR spectrum for the Jeffamine D-4000 based HPHUs can be found in **Figure S4** and **Figure S5** in Section 2 of the Supporting Information.

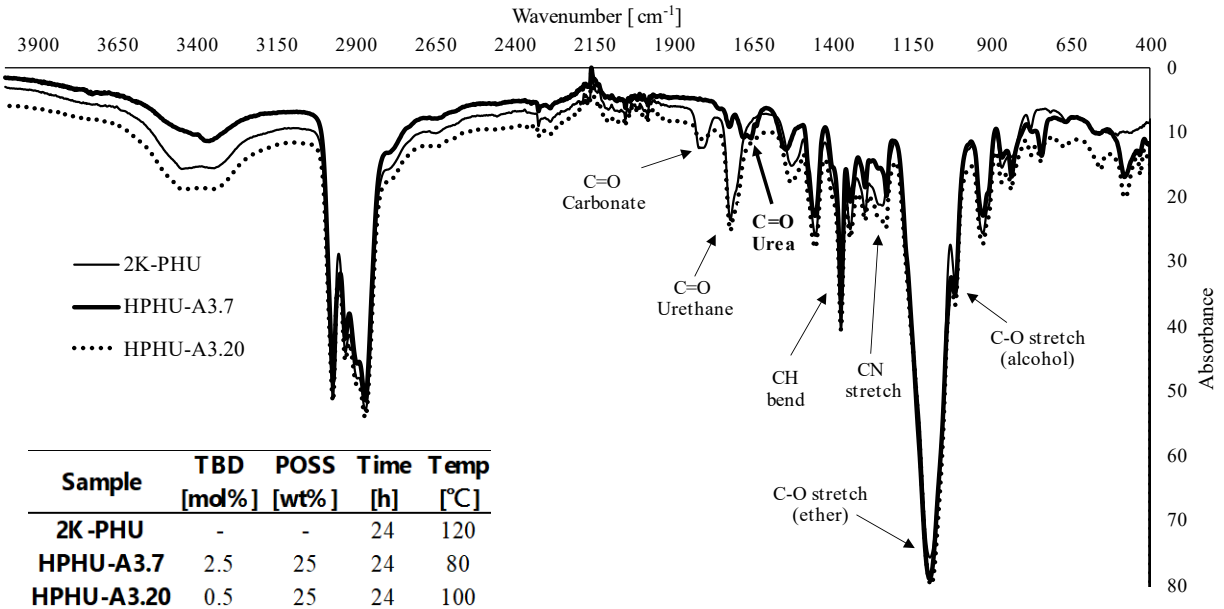

Sample	TBD [mol%]	POSS [wt%]	Time [h]	Temp [°C]
2K-PHU	-	-	24	120
HPHU-A3.7	2.5	25	24	80
HPHU-A3.20	0.5	25	24	100

Figure 1: Normalized FTIR results for the PHU prepolymer (2K-PHU) compared to an unsuccessful HPHU synthesis (HPHU-A3.7) and a successful HPHU synthesis (HPHU-A3.20) with labeled peaks.

2.1.2 GPC Results

To further characterize the HPHUs, GPC was used to determine the number average molecular weights ($\overline{M_n}$) of the POSS modified HPHUs. This would indicate a shift in molecular weight after the addition of POSS to the PHU prepolymers and provide additional evidence if the coupling reaction was successful. **Figure 2** shows the GPC plot for the initial successful HPHU reaction (based on the FTIR results) compared to its corresponding PHU oligomer (2K-PHU_A16) with bimodal peaks. This graph shows the HPHU immediately after the reaction was completed (HPHU-A3.16) and then the same HPHU after it was left to settle out for 8 weeks and the supernatant was collected (HPHU-A3.16-TOP). The reaction conditions along with the number average molecular weight $\overline{M_n}$ and dispersity ($Đ$) are also given and show increases in the molecular weight from 3,500 g mol^{-1} for the PHU to 6,800 g mol^{-1} for the top HPHU sample. HPHU-A3.16 displays a prominent peak to the right, which corresponds to the unreacted A-POSS within the polymer mixture. After letting the sample settle, this peak disappears and a shift to the left is observed, which indicates an increase in the molecular weight. This confirms that the increase in molecular weight that is observed is not coming from unreacted A-POSS in the polymer mixture, but rather from the A-POSS being covalently bonded to the PHU. This reaction was deemed successful based on the FTIR and GPC results and thus was used for further characterization, which will be presented in the following sections.

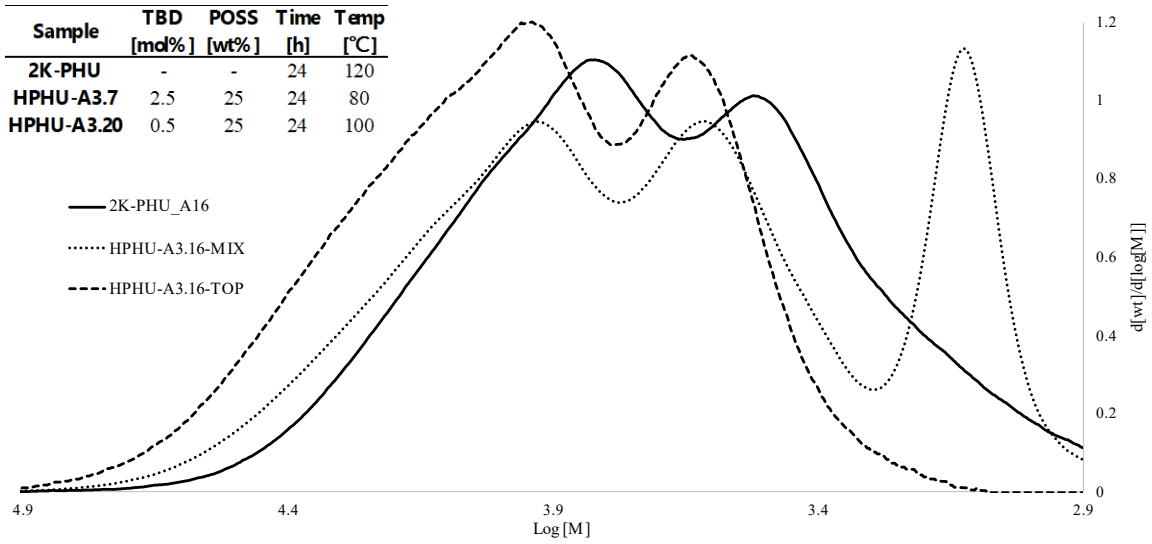

Figure 2: GPC results for HPHU-A3.16-MIX immediately after reaction (dotted) and HPHU-A3.16-TOP after left to settle for 8 weeks (dashed) as compared to 2K-PHU_A16 (solid).
[a)]Molecular weight distribution was obtained by GPC in tetrahydrofuran (THF) eluent at 40 °C and are reported with respect to PS standards.

Based on the successful synthesis of HPHU-A3.16, subsequent PHU prepolymers and HPHU materials were synthesized in the same way and are presented in **Table 1**. These reactions form the foundation of this work and are used in the subsequent curing reactions that will be further discussed in section 2.2. This table summarizes the GPC results relative to PMMA standards and gives the $\overline{M_n}$ and $Đ$ values. Overall, the results show $\overline{M_n}$ increases from the PHU to the HPHUs ranging from 2,000 – 5,000 g mol^{-1}, which corroborates the FTIR findings that the A-POSS is successfully being incorporated into the polymers. Further data for the Jeffamine D-4000 reactions is given in Section 1 of the Supporting Information.

Table 1: Average and absolute molecular weights of synthesized PHUs and HPHUs

Sample [a)]	Jeffamine	Temp [°C]	Time [h]	$\overline{M_n}$ [b)] [g mol^{-1}]	$Đ$ [b)]
Jeffamine D-2000	-	-	-	1,800	1.20
2K-PHU	D-2000	120	24	5,900	2.15
HPHU-A3.20-TOP	D-2000	100	24	7,500	1.74
HPHU-A3.21-TOP	D-2000	100	24	7,800	1.82
HPHU-A3.22-MIX	D-2000	100	24	7,400	1.77
Jeffamine D-4000	-	-	-	3,700	1.38
4K-PHU	D-4000	120	28	5,900	1.99
HPHU-A4.1-MIX	D-4000	100	48	9,300	1.58
HPHU-A4.1-MIX	D-4000	100	72	11,100	1.54
HPHU-A4.2-TOP	D-4000	100	72	10,100	1.59

a) 2K-PHU is the Jeffamine D-2000 based prepolymer and is used in the synthesis of the HPHUs that appear below it (HPHU-A3.20-A3.22). 4K-PHU is the Jeffamine D-4000 based prepolymer and is used in the synthesis of the HPHUs that appear below it (HPHU-A4.1-A4.2); **b)** Molecular weight distribution was obtained by GPC in tetrahydrofuran (THF) eluent at 40 °C and are reported with respect to PMMA standards.

2.1.3 NMR Results

^{1}H and ^{29}Si NMR experiments were also performed to obtain information about the molecular structure beyond just the functional groups. **Figure 3** provides the predicted ^{1}H NMR spectra for A-POSS along with the labelled structure to provide context for the experimental results. **Figure 4** gives the experimental ^{1}H NMR results for the A-POSS (top), the HPHU-A3.16-TOP (middle), and the PHU prepolymer (bottom). When comparing these spectra, the HPHU has all the peaks from the PHU, but also shows peaks that correspond to the A-POSS at 0.6, 0.95, and 1.8 ppm. However, there are no peaks appearing at 2.65 ppm or 1.5 ppm (which correspond to the A-POSS) in the HPHU spectrum. The peaks at 2.65 and 1.5 ppm for the A-POSS correspond to the protons that are 1 and 2 bonds away from the amine group, respectively (peaks A and C in **Figure 3**). When the amine group is reacted, these peaks are expected to shift as the chemical environment of the protons has changed. Therefore, since all other peaks from the A-POSS are present in the HPHU spectra, but not the peaks at 2.65 and 1.5 ppm, this indicates that the amine of the A-POSS has been reacted and successfully incorporated into the HPHU. **Figure S7** in the Supporting

Information gives a ^{1}H NMR spectrum of an unsuccessful HPHU synthesis where all A-POSS peaks appear, indicating that the peaks at 2.65 and 1.5 ppm are detectable in the polymer mixture.

^{29}Si NMR was also conducted to further confirm the addition of A-POSS. This test was performed on the HPHU sample that was left to settle for over 6 weeks and only the supernatant layer was taken for analysis. GPC analysis was also performed on the same sample to ensure that no A-POSS peak was appearing. **Figure 5** gives the HMBC between ^{1}H and ^{29}Si and shows a 2D plot with the ^{1}H signal in the horizontal and the ^{29}Si signal in the vertical. The darker contours shown in this plot indicate Si elements that are detected. These appear at 0.6, 0.95, and 1.8 ppm on the horizontal ^{1}H dimension and around 65-70 ppm in the vertical ^{29}Si dimension. The resonances in the ^{1}H dimension are consistent with the results in **Figure 4**. Additionally, the chemical shifts shown in the ^{29}Si dimension are consistent with those reported for Si-O-Si POSS cages in the literature.[60] Since this sample is free from unreacted A-POSS, and the PHUs alone do not contain any Si molecules, it can be concluded that the Si detected in this plot is a result of the A-POSS that has been covalently bonded to the PHUs.

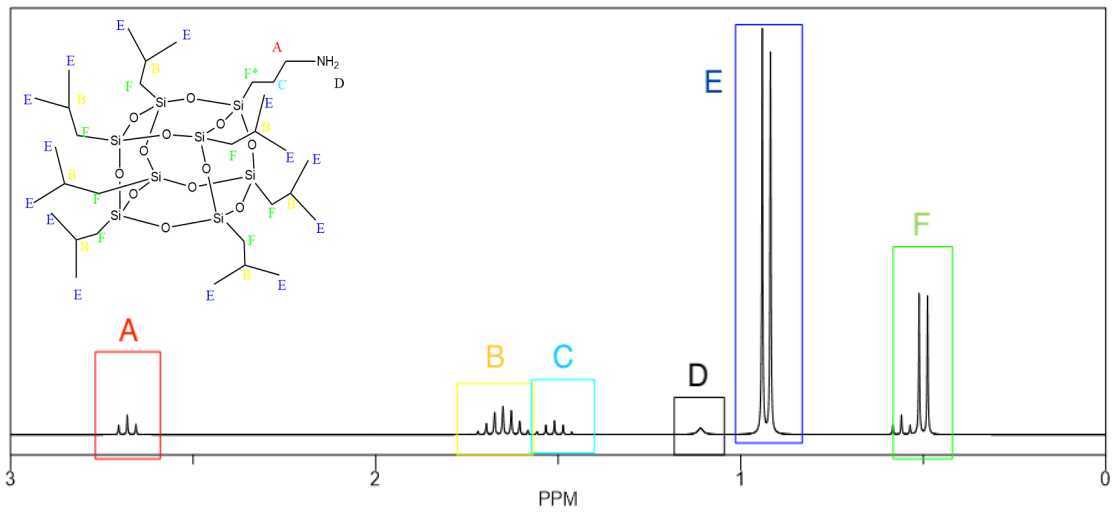

Figure 3: Predicted ^{1}H NMR spectrum for A-POSS with labelled peaks from ChemDraw.

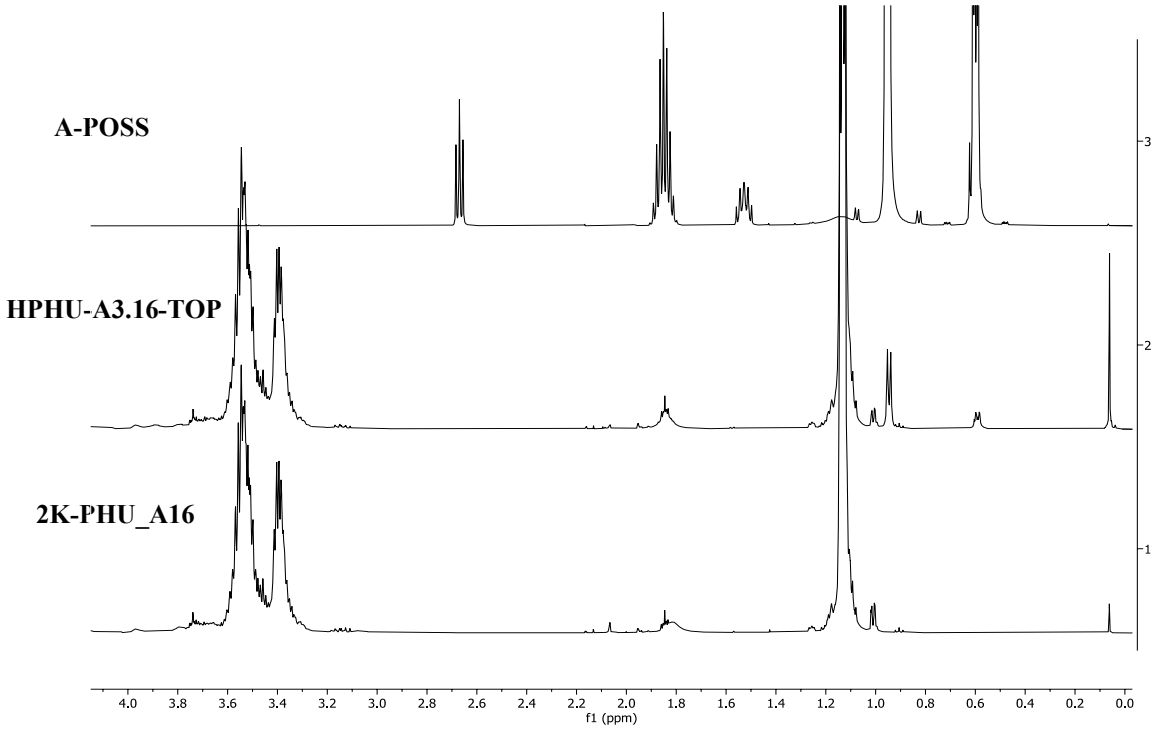

Figure 4: ^{1}H NMR results for A-POSS (top), HPHU-A3.16-TOP* (middle), and 2K-PHU_A16 (bottom) (*Corresponds to the sample given in **Figure 2**).

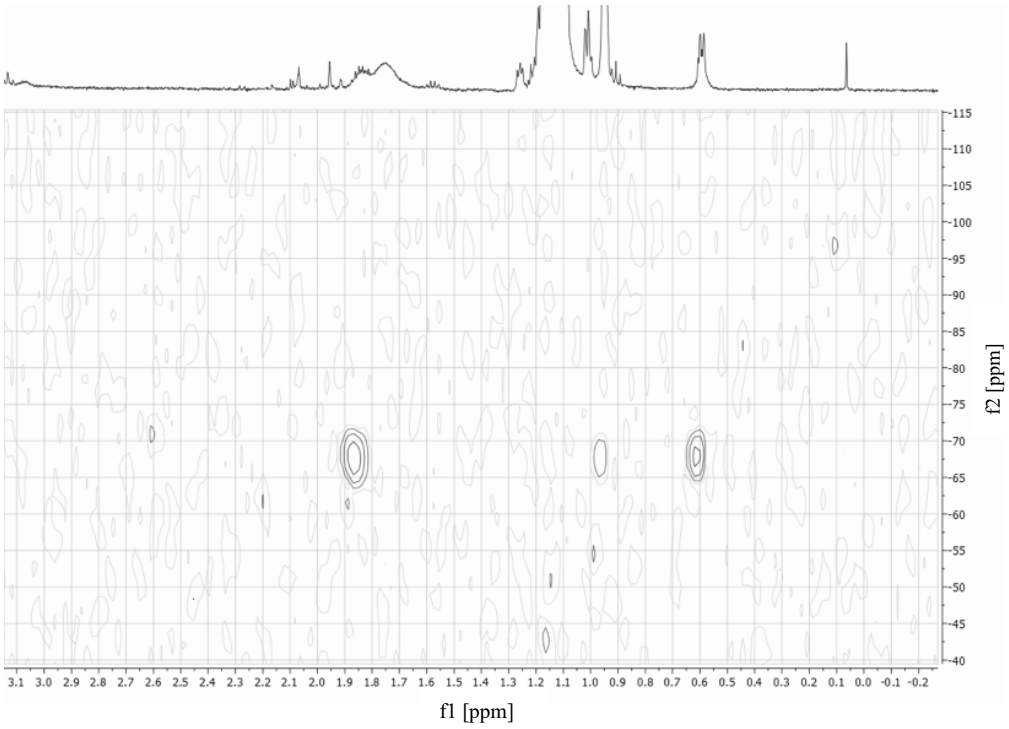

Figure 5: HMBC between ^{1}H and ^{29}Si NMR spectrum for uncured HPHU-A3.16-TOP.

2.1.4 TGA & DSC Results

TGA and DSC were performed on the HPHUs to determine the thermal properties of the polymers before final curing. **Figure 6** shows the resulting TGA plot of a PHU prepolymer compared to a HPHU with unreacted POSS in the mixture and a HPHU with no unreacted POSS. The PHU prepolymer (2K-PHU_A16) has the lowest onset degradation temperature ($T_{d,onset}$) and the steepest slope, indicating that it rapidly degrades after $T_{d,onset}$. The two HPHUs (HPHU-A3.16-TOP and HPHU-A3.16-MIX) show slightly higher thermal degradations (T_d) values and give more moderate slopes with the MIX HPHU displaying the highest T_d values. This shows that the addition of A-POSS increases the T_d with a clear increase with additional unreacted A-POSS within the HPHUs.

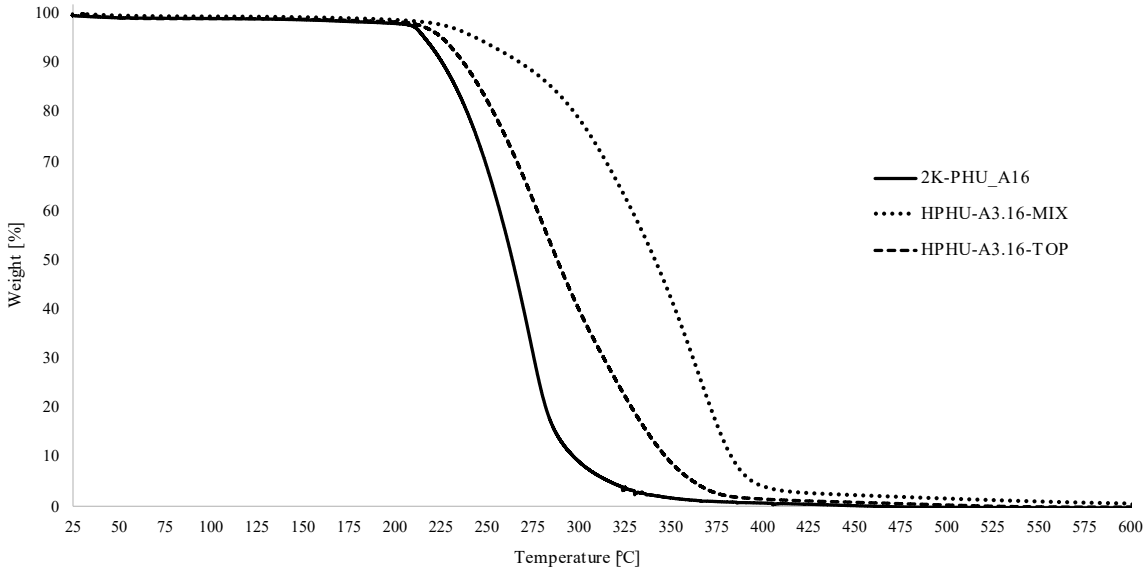

Figure 6: TGA Results for 2K-PHU_A16 and HPHU-A3.16-MIX and HPHU-A3.16-TOP.

DSC and steady shear viscosity tests were also performed to determine the glass transition temperature (T_g) and viscosities of the HPHUs and their PHU counterparts. These results are provided in **Table 2** and were conducted on the subsequent reactions that HPHU-A3.16 was based on, as given in **Table 1**. The T_g values obtained are similar and only slight deviations are observed

between the PHU and HPHUs. However, there is about a 5 °C difference between the Jeffamine D-2000 and Jeffamine D-4000 polymers. This can be explained by the difference in the chain lengths of the Jeffamine macromonomers, which affects the flexibility of the polymers resulting in different T_gs. The steady shear viscosities taken at ambient temperature and shear rates from 0.1 to 10 s^{-1} are also given in **Table 2**. The Jeffamine D-2000 based HPHUs have the highest viscosities, which is understandable as this Jeffamine is a shorter chain diamine with less flexibility and therefore a higher viscosity. Perhaps more importantly, the viscosities for all the HPHUs were higher than their PHU counterparts, demonstrating the physical change brought about by incorporating the A-POSS. The HPHU formulations are within a reasonable viscosity, making them suitable candidates to be end-capped.

Table 2: Summary of T_g and viscosity results for uncured PHU/HPHUs

Diamine	Sample	T_g [°C]	η [Pa s][a]
Jeffamine D-2000	**2K-PHU**	-61.7	9.2
	HPHU-A3.21-TOP	-62.6	35.9
	HPHU-A3.21-MIX	-61.8	44.7
Jeffamine D-4000	**4K-PHU**	-66.3	5.9
	HPHU-A4.2-TOP	-67.1	16.6

[a)]Steady shear viscosity η measured at ambient temperature and shear rates from 0.1-10 s^{-1}.

2.2 Curing Synthesis and Characterization

IPTMS was used to cap the pendant hydroxyl groups on the backbone of the polymer. This method results in a PHU backbone, end-capped with A-POSS and IPTMS attached throughout the backbone as shown in **Scheme 2**. The maximum ratio of IPTMS used was 10:1 as there are 10 -OH groups in the HPHUs (calculation provided in Section 3 of the Supporting Information). This ratio along with 5:1 ratio was investigated for the HPHUs/PHUs with Jeffamine D-2000 in the backbone. Next, a ratio of 10:1 was explored again, however with Jeffamine D-4000 in the backbone of the HPHUs/PHUs. **Table 3** gives an overview of the three sets of experiments that

have been conducted below along with gel content (*GC*) and swelling index (*SI*) results in THF, water, and toluene.

*GC*s in THF were recorded for the cured films along with corresponding *SI*s. In general, the polymers with increasing amounts of A-POSS swelled the least whereas the PHUs exhibited the highest *SI*s. This can be attributed to the hydrophobic nature of A-POSS. The third set of experiments with Jeffamine D-4000 and a 10:1 ratio of IPTMS gave highest *SI*s, which is due to the longer chain diamine as there is more surface for the THF to penetrate the polymer and cause it to swell. This highlights how changing the diamine as well as the IPTMS and POSS concentrations affects swelling of the polymer. Overall, the cured films exhibited high *GC*s with values from 87-99 %. This exceeds what has previously been reported in literature as similar linear NIPUs were found to have *GC*s around 56 %.[39] These *GC* results are comparable to branched NIPUs that have recently been reported.[37]

GC tests in water and toluene were also performed to investigate the effect POSS had on the swelling of the polymers. Due to the hydrophobic nature of POSS, swelling in water is expected to be reduced for the HPHUs compared to the PHUs. Additionally, POSS is known to swell in toluene[61] and thus, the *SI* in toluene is expected to be greater for the HPHUs compared to the PHUs. The results, given in **Table 3**, agree with the hypothesis as the *SI* in water for the HPHUs (experiment No.2 and No.9) is much less than that for the PHUs (experiment No.1 and No.7). Conversely, the *SI* in toluene is greater for the HPHUs as compared to the PHUs. This further confirms the successful incorporation of A-POSS into the polymer network as sample No.2 TOP HPHU, which has no unreacted A-POSS, exhibits the swelling behaviours of POSS rather than that of the neat PHUs. Moreover, these results also show very low *SI*s in water for both HPHUs, indicating that they repel water, which is a desired property for PU sealants.

Next, contact angle testing was performed on sets 1 and 2 of the cured HPHUs. This test gives insight on the hydrophobicity of the films and shows how water interacts on the film's surface. In general, the higher the contact angle, the more hydrophobic the sample is with contact angles above 90° considered hydrophobic. Each sample was tested at 5 different locations on the film and the results were averaged to give a single mean value for the contact angle. **Table 3** gives a summary of these results. Besides the first sample, all films were at or very close to 90°, thus making them slightly hydrophobic. These results concur with the *GC* tests in THF and the water and toluene swelling that was completed as it further demonstrates the addition of A-POSS increases the hydrophobicity of the polymer.

Table 3: Summary of Silane End-Capping Reactions

Set	No.	Sample [a]	Jeffamine	IPTMS: PHU	Contact Angle [°]	*GC* in THF [%]	*SI* in THF [%]	*GC* in H_2O [%]	*SI* in H_2O [%]	*GC* in Tol [%]	*SI* in Tol [%]
	1	**2K-PHU-IPTMS-1**	D-2000	10:1	72.6	99	123	>99	58	>99	121
1	**2**	**A3.20-TOP-IPTMS**	D-2000	10:1	91.9	92	112	>99	10	99	185
	3	**A3.20-MIX-IPTMS**	D-2000	10:1	90.1	87	104	-	-	-	-
	4	**2K-PHU-IPTMS-2**	D-2000	5:1	-	93	149	-	-	-	-
2	**5**	**A3.21-TOP-IPTMS**	D-2000	5:1	-	90	160	-	-	-	-
	6	**A3.22-MIX-IPTMS**	D-2000	5:1	-	90	155	-	-	-	-
	7	**4K-PHU-IPTMS**	D-4000	10:1	87.0	98	180	>99	32	>99	123
3	**8**	**A4.2-TOP-IPTMS**	D-4000	10:1	89.2	91	188	-	-	-	-
	9	**A4.1-MIX-IPTMS**	D-4000	10:1	87.2	87	138	>99	9	91	174

[a)]2K-PHU-IPTMS-1 was synthesized with the corresponding 2K-PHU prepolymer and a 10:1 ratio of IPTMS and is used for comparison to the A-POSS modified HPHUs. Similarly for the 2K-PHU-IPTMS-2, however a 5:1 ratio of IPTMS was used. Finally, 4K-PHU-IPTMS was synthesized with the corresponding 4K-PHU prepolymer and a 10:1 ratio of IPTMS.

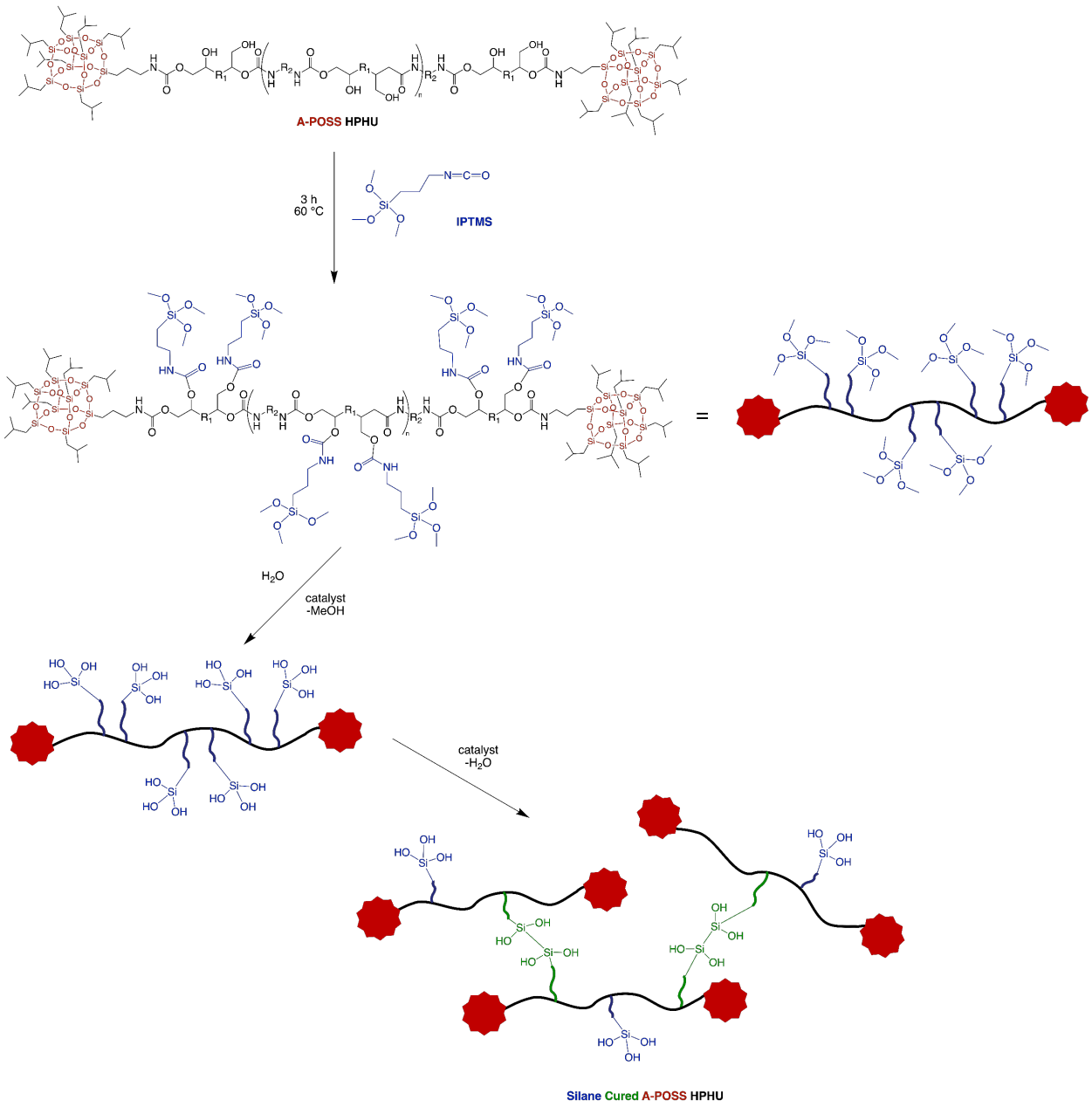

Scheme 2: Synthesis of cured A-POSS HPHU films. R_1 represents the chain of the cyclic carbonate monomer and R_2 represents the chain of the amine monomer; the number of polymer units, n=3. Note that the curing occurs through the condensation of the silane groups while using moisture in air. The products having been end-capped with siloxy groups will become moisture curable, leading to cross-linked species.

2.2.1 FTIR Results

FTIR was used to verify that the IPTMS was reacting with the pendent -OH groups of the polymer backbone. **Figure 7** shows the FTIR spectrum for the PHU prepolymer compared to the

silane modified IPTMS:PHU at a 10:1 ratio. This spectrum shows that the peak for the CC end groups of the PHU prepolymer at 1800 cm^{-1} is unchanged, while the urethane peak at 1720 cm^{-1} is increased. Moreover, there is also an increase in the NH bend at 3330 cm^{-1} and 1530 cm^{-1} as well as a decrease in the OH peak at 1012 cm^{-1}. This confirms that IPTMS is not reacting with the CC groups but is reacting with the OH groups to form additional urethane bonds. Overall, these results show that IPTMS is successfully being introduced into the polymer matrix to give moisture curable HPHU films.

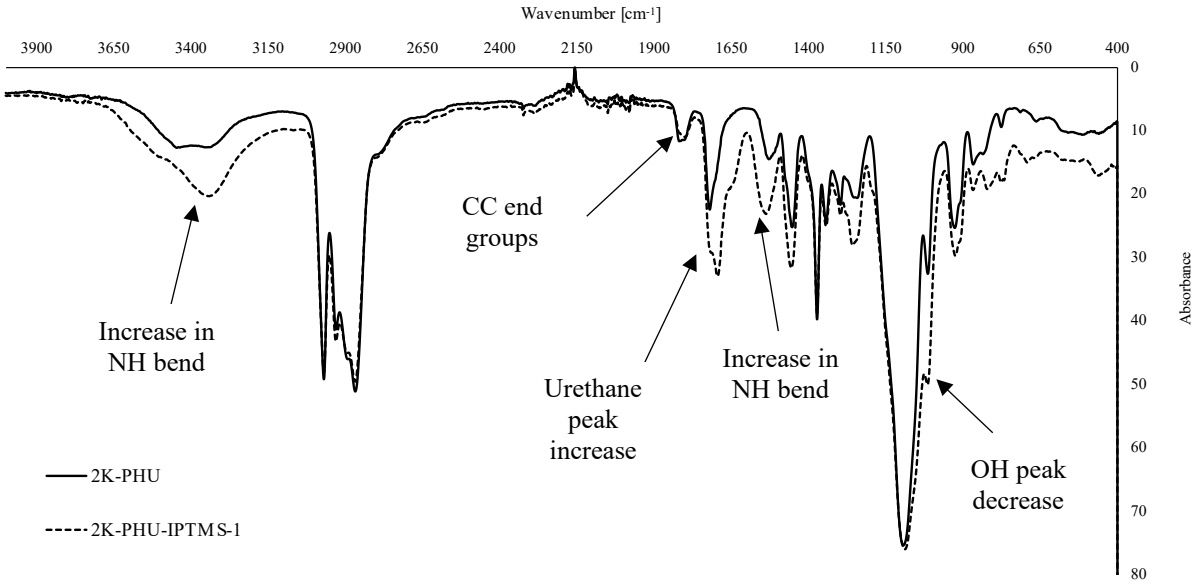

Figure 7: FTIR spectrum of 2K-PHU prepolymer (solid) compared to cured 2K-PHU-IPTMS-1 (dashed) at 10:1 ratio IPTMS:PHU.

2.2.2 Curing Kinetics

Curing kinetic studies were performed on the PHU and HPHUs capped with IPTMS to determine the gel time, or when the film began to form. The tin-based catalyst was added to the reactor after the IPTMS reaction to accelerate the curing reaction at ambient conditions. Without the catalyst, the curing reaction took well over 6 weeks to fully cure, where curing overnight was observed with the catalyst. Both the Jeffamine D-2000 and D-4000 based PHUs and HPHUs were

studied, and all reactions had gel times under 1 h and fully cured films were observed in 24 h. This is similar to previously reported curing times for HPHUs within 24 h[4, 36, 37] and is within the curing time of 13-36 h for typical PU sealants.[62] Graphical representations of the curing kinetics are provided in **Figure S9** and **Figure S10** in Section 3 of the Supporting Information.

2.2.3 TGA & DSC Results

TGA and DSC were performed on the cured polymers to determine the thermal properties of the films. Experiment No.9, the Jeffamine D-4000 MIX HPHU, displayed the highest thermal stability with T_ds at 1 % and 10 % weight loss of 197.9 °C and 299.3 °C, respectively. However, the differences between the T_ds for the cured polymers were minimal and all films displayed adequate thermal stability. Nonetheless, the mixed HPHUs, both cured and uncured, gave the best performance in terms of thermal degradation. An increase of 19 % was observed for T_d values at 10 % weight loss for the uncured HPHUs compared to the PHUs. Similarly, an increase of 0.4 % for the T_d at 10 % weight loss for the cured HPHUs compared to the PHUs was recorded. Thus, it can be concluded that the addition of A-POSS enhances the thermal stability of the PHUs. DSC was performed on the cured films and the resulting T_g values were similar to their uncured counterparts. A low 2 °C difference was observed between the cured PHU and HPHUs. This small increase could be due to the addition of POSS cages at the nanometer level, which restrict the motion of macromolecular chains as shown in other POSS-modified polymers.[32, 33] The low T_g values can be attributed to the long chain diamines, as they provide flexibility and make up most of the polymer, thus dominating the thermal behavior. Further data is available in Section 3 of the Supporting Information.

2.2.4 Tensile Testing

Tensile testing was performed to elucidate the mechanical properties of the cured HPHU films. This was useful in determining if adding POSS to the PHUs added strength to the polymer network, which was one of the main goals of this work. The Young's modulus (E), elongation at break ($EB\%$), and tensile strength at break (σ_{max}) were investigated. To begin, 5-6 dog bone shaped cut-outs were taken for each sample to be analyzed, and the results were averaged to give a single mean value. The results are summarized in **Table 4**. Additionally, the tensile properties for an isophorone diisocyanate (IPDI) based PU with a PPG-diol of similar molecular weight to Jeffamine D-2000 are also given for comparison. The first set of samples displays high Young's modulus, good tensile strength, but lower elongations at break. For example, experiment No.3: MIX HPHU, has the highest Young's modulus of 5.9 MPa but the lowest elongation at break at 16.5 %. This is likely due to the unreacted A-POSS remaining in the HPHU during the curing reaction, which imparted brittleness to the material. Experiment No.2: TOP HPHU gives a good balance of properties with an increase in all three variables from the PHU in addition to a two-fold increase in the tensile strength compared to the PU. However, the elongation at break is still lower.

The next set of samples with a 5:1 ratio of IPTMS and using Jeffamine D-2000 yielded lower Young's modulus and tensile strength, but similar elongations at break compared to the first set. The increase in strength from the PHU to HPHU was still observed, however the increase between the MIX HPHU and TOP HPHU is much smaller as compared to the first set of samples. The decrease in the strength from the 5:1 compared to the 10:1 samples was expected; however it was hypothesized that the elongation at break would be increased. This was not necessarily the case and interestingly the MIX HPHU gave the highest elongation at break, where previously it was the

lowest. Overall, this set has unsatisfactory results as similar properties are observed in experiment No. 1 which has no A-POSS.

Finally, the third set of samples with a 10:1 ratio of IPTMS: and using Jeffamine D-4000, gave the highest elongations at break and comparatively good tensile strength. The increase in elongation can be attributed to the longer chain diamine, Jeffamine D-4000, which we employed for this very reason. Very good tensile strength was also observed for this set and there was again an increase from the PHU to the HPHUs showing that the A-POSS is adding strength to the polymer network. Experiment No. 9: MIX HPHU had the second highest elongation at break and the highest tensile strength of all the samples studied, making it the best performing HPHU with a good mix between strength and elasticity. When comparing this to the PU, the tensile strength is doubled and the elongation at break falls well within the bounds, albeit on the lower end. Overall, experiment No.9: MIX HPHU exceeds the bench-mark PU on tensile strength while approaching it on elongation at break. An example stress-strain curve is given in Section 3 of the Supporting Information.

Table 4: Tensile Testing Results

Set	No.	Ratio [a] / Diamine [b]	Sample [c]	Youngs Modulus [MPa]	Tensile Strength [MPa]	Elongation at Break [%]
	0	-	PU	-	0.6 ± 0.2	60 ± 25
1	**1**	10:1 Jeff 2000	PHU	2.4 ± 0.27	0.66 ± 0.12	24.8 ± 4.0
	2		TOP HPHU	3.7 ± 0.24	1.17 ± 0.04	28.2 ± 5.2
	3		MIX HPHU	5.9 ± 0.80	1.09 ± 0.04	16.5 ± 6.5
2	**4**	5:1 Jeff 2000	PHU	1.7 ± 0.14	0.55 ± 0.09	29.6 ± 6.4
	5		TOP HPHU	2.4 ± 0.34	0.76 ± 0.04	28.1 ± 4.0
	6		MIX HPHU	2.6 ± 0.20	0.91 ± 0.16	32.8 ± 7.0
3	**7**	10:1 Jeff 4000	PHU	2.0 ± 0.18	0.82 ± 0.11	36.4 ± 7.0
	8		TOP HPHU	1.7 ± 0.12	0.84 ± 0.11	46.1 ± 7.5
	9		MIX HPHU	3.1 ± 0.19	1.32 ± 0.14	41.6 ± 5.3

[a] Molar ratio of IPTMS:(H)PHU. Calculation is provided in Section 3 of Supporting Information; [b] Diamine used to formulate the PHU and HPHUs; [c] Sample names are shortened for ease of reading; full sample names are given in **Table 3**.

2.2.5 SEM & TEM Results

Scanning electron microscopy (SEM) and transmission electron microscopy (TEM) were used to determine the topography of the cured samples and elucidate the distribution of the POSS within the HPHU. TEM was used for the cured PHU bearing no POSS (4K-PHU-IPTMS) and the results are shown in **Figure 8**. TEM was possible for this sample due to the homogenous nature of the neat PHU, as shown in the micrographs with the 20 nm and 2 µm scale bars. Point analysis on this sample revealed the elemental makeup and showed a small Si peak. Since there is no Si in the backbone of this polymer, the Si can be attributed to the isocyanate silane used in the curing reaction. It can also be concluded from the TEM images that the Si is evenly dispersed throughout the film and the isocyanate silane did not agglomerate during the curing reaction. TEM examination of POSS containing HPHU cured films were inconclusive as the POSS domains were too large and was detached from the matrix during the microtoming preparation step. These results are shown in **Figure S15** in Section 3 of the Supporting Information.

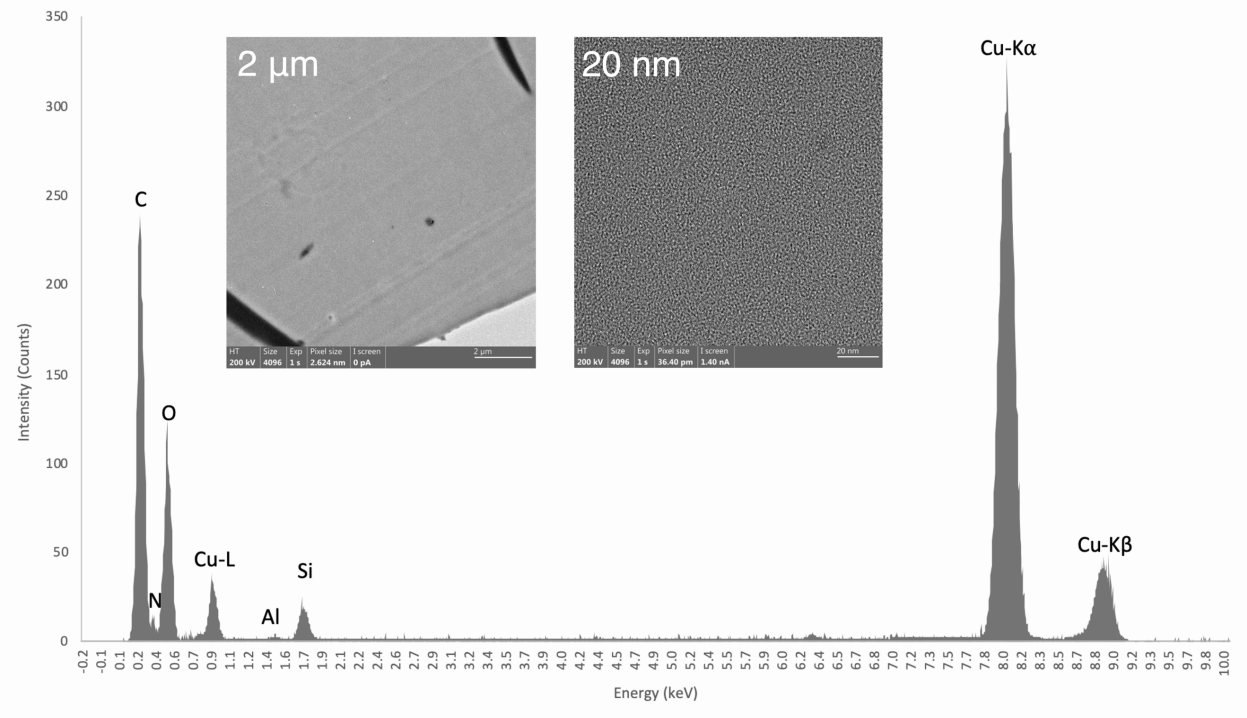

Figure 8: TEM point analysis on 4K-PHU-IPTMS with images at 20 nm and 2 μm.

SEM was run on the cured HPHU containing POSS (A4.2-TOP-IPTMS) and the results are shown in **Figure 9** and **Figure 10**. This method allowed for thicker slices to be cut during the microtoming process compared to TEM, allowing for a more accurate depiction of the topography. **Figure 9** shows the original SEM image obtained on the left and displays a non-homogenous film with agglomerates clearly visible. Elemental mapping analysis was performed to determine the nature of the agglomerates and the image on the right shows the Si analysis (additional data provided in **Figure S12** and **Figure S13** in Section 3 of the Supporting Information). This image confirms that the agglomerates are mostly comprised of Si and that there is Si dispersed throughout the film as well. Therefore, it can be concluded that the agglomerates in the film are POSS, which agrees with other studies that have reported the tendency of POSS to form aggregates.[63-65] Point analysis was also completed on this film and is given in **Figure 10**. EDS Spot 1 was taken from a point in one of the agglomerates where EDS Spot 8 was taken from a smooth surface of the film. As expected, the elemental analysis for EDS Spot 1 shows an Si peak with the strongest intensity where EDS Spot 8 shows a much lower Si peak. The results for EDS Spot 8 are comparable to the TEM results given in **Figure 8** for the neat PHU, which further confirms that the aggregates displayed in the SEM images are from the POSS end-groups aggregating in the HPHU. Future work could be focused on improving the dispersion of the POSS within the films by using alternative mixing methods. This could potentially lead to improved mechanical properties as the POSS would be reinforced throughout the polymer network, thus increasing the strength. Additionally, a higher elongation at break could also be obtained as the POSS agglomerates likely cause stress points throughout the film and impart brittleness. Therefore, improving the dispersion

of POSS would eliminate these stress points and increase the elongation of the film while maintaining good mechanical strength.

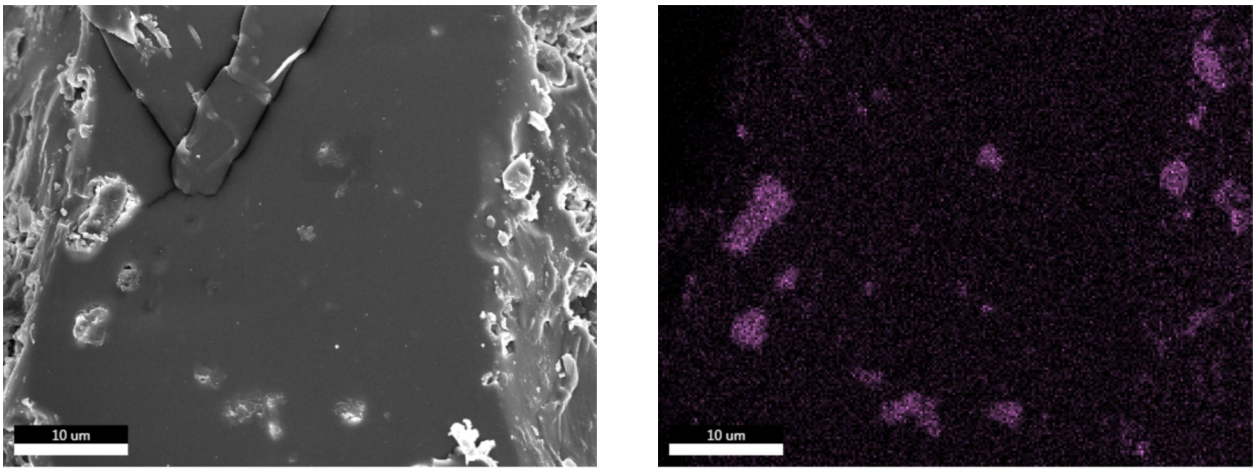

Figure 9: SEM analysis of A4.2-TOP-IPTMS **(a)** original SEM image of sample area **(b)** Si mapping analysis image.

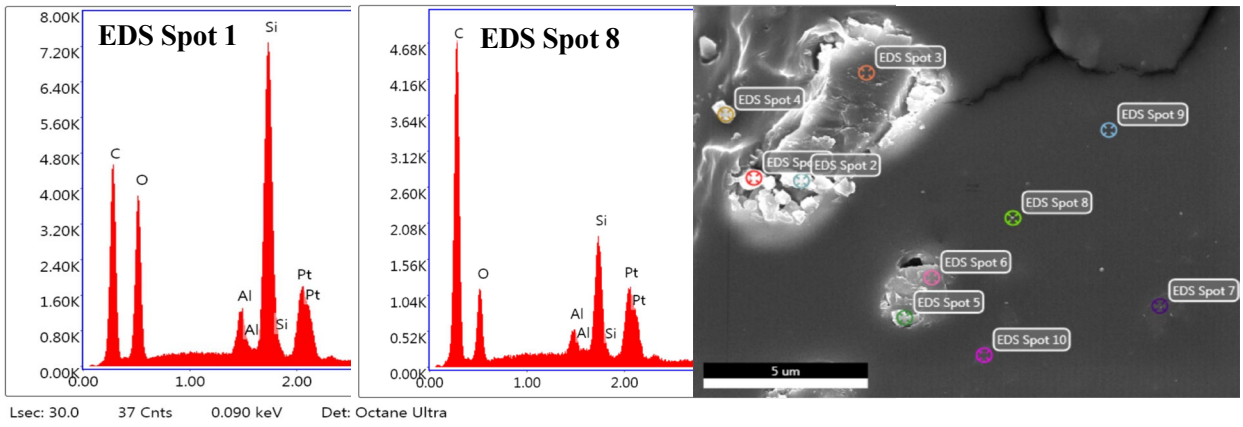

Figure 10: SEM point analysis of A4.2-TOP-IPTMS at two different points on the sample.

3. CONCLUSIONS

The main objective of this work was to formulate a POSS-modified HPHU material that had improved mechanical and thermal properties compared to its PHU counterpart and was also comparable to typical PU sealants. PHU prepolymer benchmarks were synthesized to have CC end groups which were functionalized subsequently with an amino POSS (A-POSS) to obtain a telechelic HPHU resin. POSS was covalently bonded to the polymer and not just mixed like an additive, which was proven by using FTIR, GPC, and NMR analysis. The HPHUs exhibited higher thermal degradation temperatures with increasing POSS concentration compared to their PHU counterparts.

Further functionalizing the HPHU resin with moisture curable moieties enabled polymer cross-linking at ambient conditions. Since the polymer was already end-capped with POSS, the pendant primary and secondary hydroxyl groups in the backbone of the polymer were leveraged for this curing reaction, using an isocyanate-functional silane to cap the pendant hydroxyl groups to obtain a final cured film. After a series of experiments, FTIR confirmed the successful incorporation of the IPTMS into the HPHUs with no unreacted isocyanates left in the films. Furthermore, gel content, water and toluene swelling, and contact angle tests all showed improved crosslink density and hydrophobicity of the POSS-modified HPHUs compared to benchmark PHUs. Although thermal properties of cured films improved mildly, significant improvements in mechanical properties were observed. When compared to a conventional PU, the POSS-modified HPHU exhibited a tensile strength at break that was twice as high while possessing comparable elongation at break.

However, it is important to point out the obvious drawback that was presented in this work. Though an HPHU was successfully synthesized without the use of isocyanates, in the subsequent

curing reaction, an isocyanate silane was introduced to place the moisture curable groups in the resin. It is ironic that in the pursuit to obtain a curable HPHU film, an isocyanate was added to a NIPU formulation. The reason for using the isocyanate-functional silane was to capitalize on its reactivity to the pendant hydroxyl bonds in the PHU. It should be noted that the maximum amount of isocyanate silane never exceeded 19 wt%, which is much lower than when it is used as a monomer for typical PUs. Perhaps using an approach that reacts carboxylic acid-functionalized silica particles might be a more attractive curing partner with the PHUs than the isocyanate functional silane. In summary, there is a wide variety of options to be able to further optimize the POSS-terminated additive HPHUs presented in this work, and we presented an approach to obtain HPHU films using POSS as a filler to improve mechanical properties.

4. EXPERIMENTAL SECTION

4.1 Materials

Diglycerol (DIG, ≥80% α,α, impurities consist of mono-, α,β-di-, β,β-di, and triglycerol) was obtained from Tokyo Chemical Industry (TCI). Dimethyl carbonate (DMC, ≥99%, anhydrous) and sodium methoxide (SOM, 95%, anhydrous powder) were purchased from Sigma-Aldrich and Acros, respectively. Ethyl acetate (EtOAc, certified grade), tetrahydrofuran (THF, HPCL grade), and dimethyl formamide (DMF, HPLC grade) were purchased from Fisher Scientific. Water purified by a reverse osmosis process (pure H_2O) was provided by the McGill Chemical Engineering Department. The diamines used in this work include Jeffamine D-2000 (poly(propylene glycol) bis(2-aminopropyl ether)) with $\overline{M_n}$ = 2000 g mol^{-1} (Aldrich), and Jeffamine D-4000 with $\overline{M_n}$ = 4000 g mol^{-1}. Aminopropyl isobutyl POSS (A-POSS) (AM0265) and Nanosilica Dispersion Epoxy POSS (E-POSS) (EP4F09.01) were purchased from Hybrid Plastics. The catalyst 1,5,7-triazabicyclo[4.4.0]dec-5-ene (TBD) used in this work was provided by Sigma-Aldrich. 3-isocyanatopropyl(trimethoxy)silane (IPTMS) and a proprietary tin-based catalyst (could be replaced by TBD) were provided by ADFAST Corp. Deuterated dimethyl sulfoxide (DMSO-d_6) and deuterated chloroform ($CDCl_3$) were provided from Sigma-Aldrich. DAMO or *N*-(2-aminoethyl)-3-aminopropyltrimethoxysilane was also purchased from Sigma-Aldrich. All the chemicals were used as received.

4.2 Experimental Methods

4.2.1 DGC Synthesis

The synthesis of DGC was based on optimized procedures reported by Younes *et al.*[36] First, DIG (30.0 g) is weighed and added into a two-neck round bottom flask equipped with a stir bar. Next, DMC is added at a 10:1 molar ratio of DMC:DIG (162.6 g). Finally, potassium carbonate is

added as a catalyst at 0.5 wt% of the DIG (0.15 g). This mixture is then sealed with septa, added into an oil bath, and purged with nitrogen for 15 minutes. After this, the oil bath is heated to 75 °C and the mixture is allowed to react for 24 h under magnetic stirring.

Once this reaction is complete, the mixture is filtered with a vacuum pump to remove any remaining catalyst, DMC and methanol formed during the reaction. The filtrate is left to strip under air for approximately 16 h until the liquid volume is reduced to about 50 mL. After this time, 60 mL of refrigerated reverse osmosis (RO) water is then added along with a stir bar and left to mix for 2 h. During this time, any impurities are leached into the RO water, while the DGC is crystallized from the solution. This mixture is then filtered again with a vacuum pump and the precipitated powder is collected and transferred into a beaker. The beaker is then charged with EtOAc (30 mL) and a stir bar was added and the contents mixed for an additional 30 minutes to remove any remaining impurities. Finally, this mixture is filtered again with a vacuum pump and the purified DGC powder is collected into a tin dish and topped with aluminium foil that was poked with small holes to allow any remaining volatiles to evaporate. This dish is then left to dry overnight in a vacuum oven to remove any remaining EtOAc. Once drying is complete, the final product is obtained. However, a small amount of DGC powder is first dissolved into DMSO-d6 to perform ^{1}H NMR analysis to compare to a known pure sample of DGC to confirm that the synthesis was successful, and the product is clean from impurities. Once confirmed, the DGC powder is stored in glass vials to be used for subsequent prepolymer synthesis.

4.2.2 Prepolymer Synthesis

The prepolymer reaction was also based on procedures by Younes *et al.*[36] DGC is mixed with a diamine (Jeffamine D-2000 and Jeffamine D-4000 were used in this work) at different ratios depending on the functional groups that are desired. To obtain a prepolymer with amino

functionality, an excess of Jeffamine is used at a 60:40 ratio. Conversely, to obtain a prepolymer with CC functionality, an excess of DGC is used at a 55:45 ratio. These mixtures are placed into a three-neck round-bottom flask reactor with a stir bar, sealed with septa, and then purged with nitrogen for 15 minutes. During this time, the reactor is submerged into an oil bath heated to 120 °C via a temperature controller and thermocouple and allowed to react for 24 and 28 h for the Jeffamine D-2000 and Jeffamine D-4000 PHUs, respectively. After this, the resulting polymer is collected and stored at room temperature in glass vials for subsequent reactions.

4.2.3 Hybrid PHU Synthesis

To synthesize the POSS terminated hybrid polymer, a prepolymer with CC end groups is required to react with the amino functional POSS. Therefore, the prepolymer is first synthesized with DGC in excess at a 55:45 ratio with Jeffamine D-2000 and is referred to as 2K-PHU. After this, the 2K-PHU is weighed and added to the reactor and a stoichiometric amount (2 mol of A-POSS for 1 mol of 2K-PHU) is also added. Since the reactivity of CCs to amines is slow, a low concentration of catalyst is also added into the reaction to promote the ring-opening polymerization of the CC with the amine. The catalyst used is 1,5,7-triazabicyclo[4.4.0]dec-5-ene (TBD) and is added at 0.5 mol%. This mixture was heated to 100 °C and allowed to react for 24 h. After this time, the resulting HPHU was collected and stored in 20 mL glass vials where any unreacted A-POSS was left to settle out of the mixture. The A-POSS is a fine white powder, therefore the processes of settling took about 4-6 weeks before the top polymer could be collected for analysis and subsequent reactions. To aid in this process, a Thermo Scientific Sorvall Legend RT+ swing-bucket centrifuge was also used at a force of 3000 g for 1 h. A second prepolymer was also synthesized with Jeffamine D-4000 with DGC in excess at a 55:45 ratio and is referred to as 4K-

PHU. The exact same steps were taken to prepare a second HPHU with the 4K-PHU prepolymer, however it was allowed to react for 72 h at 100 °C.

4.2.4 Silane Curing Synthesis

Once the hybrid polymer is free from unreacted POSS, it is weighed and added into a reactor with varying amount of IPTMS. IPTMS is added stoichiometrically to react with the pendant hydroxyl groups in the backbone of the PHU.

Ratios of 10:1, 8:1, 5:1, 4:1, and 2:1 of IPTMS to HPHU were explored. The ratio of 10:1 was the maximum, where all hydroxyl groups would be reacted with an isocyanate group and 2:1 was the minimum where only two hydroxyl groups would be reacted. Once the ratio was selected, the appropriate amount of IPTMS was weighed and added to the reactor with the HPHU and allowed to react for 3 h at 60 °C. After this time, the reaction was removed from heat and the tin-based catalyst (0.02 wt%) was mixed into the solution for 2 minutes. The mixture was then poured onto a Teflon sheet and spread into a thin film to allow the final hybrid material to cure in ambient conditions.

4.3 Characterization Methods

4.3.1 Gel Permeation Chromatography (GPC)

The PHU prepolymers and the HPHUs containing POSS were dissolved in HPLC grade THF at a concentration of 2.5 g L^{-1} in a 1-dram glass vial. The samples were measured on a Waters Breeze instrument with HLPC-grade THF as an eluent at a flow of 0.3 mL min^{-1}, powered by a Waters 1515 Isocratic HPLC pump. The instrument has three Waters Styragel HR columns (HR1 with a molecular weight measurement range of 10^2 to 5×10^3 g mol^{-1}, HR2 with a molecular weight measurement range of 5×10^2 to 2×10^4 g mol^{-1}, and HR4 with a molecular weight measurement range of 5×10^3 to 6×10^5 g mol^{-1}), a (RI 2414) refractive index detector, and a

guard column. An injection of 10 μL of dissolved PHU or HPHU was passed through the columns, which was kept at a temperature of 40 °C. The samples elution time was 60 minutes. The molecular weights were determined relative to PMMA calibration standards from Varian Inc. (ranging from 682 to 2,520,000 g mol^{-1}). The number average molecular weight ($\overline{M_n}$), weight average molecular weight ($\overline{M_w}$) and dispersity ($Đ$) of the samples were reported relative to the PMMA standards.

4.3.2 FTIR

FTIR was performed on all PHU prepolymers and HPHUs as well as most cured samples. A Thermo Fisher Scientific Nicolet iS50 FTIR spectrometer equipped with a single bounce diamond attenuated transmission reflectance and a diamond DLaTGS detector was used. First, a background reading was performed on a clean diamond free from any sample to obtain an accurate baseline. The sample, either liquid or solid, was then placed on the diamond detector to fully cover it and was gently pressed to ensure adequate contact. A total of 32 scans were recorded for each sample over the range 4000-400 cm^{-1}. The results were plotted with respect to % transmittance and analyzed with Thermo Fisher Scientific Omnic software.

4.3.3 NMR Spectroscopy

NMR was performed on both the PHU prepolymers and the HPHU materials. Approximately 5 mg of polymer was dissolved in $CDCl_3$ (2 mL) and 0.5 mL of this solution was transferred into an NMR tube. DGC was also analyzed via NMR; however, it was dissolved into a solution of DMSO-d_6. All samples were run with ^{1}H NMR and only a select few HPHU samples were run with ^{29}Si NMR to confirm the presence of POSS in the samples.

^{1}H NMR

Proton NMR experiments were conducted on a Bruker 500 MHz NMR Spectrometer in 1D using 16 scans. The analysis was completed at room temperature with a zg30 pulse sequence. The resulting spectra was analyzed and interpreted using Mestrelab MNova software.

^{29}Si NMR

^{29}Si NMR experiments were also conducted on a Bruker 500 MHz NMR Spectrometer using a heteronuclear multiple bond correlation (HMBC) between ^{1}H - ^{29}Si. The signal first excites on ^{1}H, and then transfers the signal to ^{29}Si to detect ^{29}Si in the vertical (indirect or f1) dimension of a 2D experiment, and then transfer back to ^{1}H for detection in the horizontal (direct or f2) dimension. The resulting spectra was analyzed and interpreted using Mestrelab MNova software.

4.3.4 Thermogravimetric Analysis (TGA)

Thermogravimetric analysis (TGA) is used to determine the thermal degradation of the PHU prepolymers and A-POSS HPHUs to discern any differences between the two. A TA Instruments Discovery 5500 thermogravimetric analysis instrument was used. First, a small platinum pan is cleaned with a blow torch to remove any residue from previous samples, then weighed and tared. Next, approximately 5 mg of sample is added into the pan and weighed by the machine to get an exact measurement. Finally, the sample is loaded into the furnace chamber where it is heated from ambient temperature to 600 °C at a rate of 10 °C min^{-1} under a nitrogen atmosphere. The resulting thermal degradation plot was analyzed with TA Instruments Trios software in which the onset degradation temperature ($T_{d,onset}$) and 10 % degradation temperature ($T_{d,10\%}$) were calculated.

4.3.5 Differential Scanning Calorimetry (DSC)

Differential Scanning Calorimetry (DSC) was used to determine the glass transition temperature (T_g) of the PHU prepolymers and A-POSS HPHUs. A TA Instruments Discovery 2500

DSC instrument was used. A standard hermitic aluminium pan is first weighed and tared, then 5-10 mg of a sample is added. The pan is then sealed with a top using a press machine and weighed again to determine the sample weight. The pan is loaded into the apparatus and analyzed in a nitrogen environment. Heat-cool-heat experiments were performed to ensure that the resulting T_g is unaffected by the thermal history of the polymer. This experiment is performed by heating the sample to 120 °C at a rate of 10 °C min^{-1}, then cools to -90 °C, and finally heats the sample again to 120 °C. The resulting plot was analyzed with TA Instruments Trios software and the T_g was calculated from the second heating ramp.

4.3.6 Gel Content

Gel content (*GC*) was only performed on cured samples. Three square samples, approximately 10x10 cm were cut from a cured film and each placed into pre-weighed 20 mL vials. The vials were then weighed again to determine the initial weight of the cured samples. Finally, THF (10 mL) was added to the vials to submerge the samples, which were then capped and left undisturbed for one week to soak. After this time, the samples were filtered, and the remaining solid sample was immediately weighed to determine the swollen mass. The samples were then transferred back to their respective 20 mL vials and topped with aluminium foil perforated with small holes. The vials were then placed into a Fisher Scientific Isotemp® vacuum oven model 281A connected to a Welch® 8917 vacuum pump. The pressure inside the oven reaches approximately -30" gauge and the samples were left to dry at room temperature overnight for 15 h. Once dry, the samples were removed from the oven and weighed again to determine the dry mass of the samples. The average of the three samples was taken and reported as a mean value to give a more accurate value for the *GC*. The *GC*, and swelling index (*SI*) are given below in **Equation 1** and **2**, respectively.

(1) $$GC(\%) = \left(\frac{W_f}{W_i}\right) \times 100$$

(2) $$SI(\%) = \left(\frac{W_s - W_i}{W_i}\right) \times 100$$

Where W_f is the final weight of the dried sample, W_i is the initial weight of the sample, and W_s is the weight of the swollen sample.

4.3.7 Water and Toluene Swelling

Water and toluene swelling was also only performed on cured samples. Three square samples, approximately 10x10 cm were cut from a cured film and each placed into pre-weighed 20 mL vials. The vials were then weighed again to determine the initial weight of the cured samples. Finally, RO water (10 mL) or toluene was added to the vials to submerge the samples, which were then capped and left undisturbed for one week to soak. After this time, the samples were filtered, and the remaining solid sample was immediately weighed to determine the swollen/final mass. The average of the three samples was taken and reported as a mean value to give a more accurate value for the water or toluene swelling. The water and toluene absorption (*WA%*) values were calculated from **Equation 3**.

(3) $$WA(\%) = \left(\frac{W_f - W_i}{W_i}\right) \times 100$$

4.3.8 Rheology

Rheology experiments were performed on an Anton Paar MCR 302 modular compact rheometer with a CTD 450 furnace. Air flow of 1400 Nl h^{-1} was used for shaft cooling along with 850 Nl h^{-1} of air or nitrogen, depending on the experiment, to the furnace. The Anton Paar PP25 25 mm diameter parallel plate sensor is used for all steady shear viscosity and parallel curing tests. The results were analyzed with Rheocompass software connected to the rheometer.

Steady Shear Viscosity Test

A polymer sample (1 mL) is placed onto the bottom 25 mm diameter parallel plate so that it is fully covered. The top PP25 plate is then lowered to give a 1 mm gap between the plates for the sample to fill and any excess from the sides is trimmed. All experiments are performed at ambient conditions. The shear stress is measured at different shear rates from 0.1 to 10 s^{-1} with 21 readings over 3 min. The resulting viscosity curve is analyzed, and an average viscosity (η) is reported.

Parallel Plate Curing

Once completing a curing experiment, as outlined in section 4.2.4, the polymer (1 mL) is immediately transferred to the bottom 25 mm diameter parallel plate of the rheometer so that it is fully covered. The top PP25 plate is then lowered to give a 1 mm gap between the plates for the sample to fill and any excess from the sides is trimmed. All tests were performed at ambient conditions with the furnace doors open to expose the sample to air during the experiments. The experiments were performed at a frequency of 1 Hz and a strain of 1 % with a humidity range from 25-60 %. The instrument performed shear rheological measurement every 10 seconds recording the storage modulus (G') and loss modulus (G'') until the gel time was observed, which is when the curves intersect. Depending on the experiment, the samples were allowed to cure from 24-48 h.

4.3.9 Tensile Testing

Tensile testing is only performed on cured samples as described in section 4.2.4. Once the sample is fully cured (~1 week) on a Teflon sheet, 3-5 dog bone (ASTM D638-14) shaped bars are cut out of the film with a punch mould. The bars are then carefully measured with digital calipers for their thickness, length, and width of the middle section to an accuracy of 0.01 mm. The samples are analyzed at ambient conditions with a Shimadzu EZTest Tensile Testing machine

using WinAGS Lite software. Once the measurements are complete and entered in the software, the sample is clamped into the machine and pulled at a speed of 10 mm min^{-1}. The resulting stress strain curve is produced, in which the Young's modulus (E), elongation at break ($EB\%$), and tensile strength (σ_{max}) can be calculated. The results are averaged over at least three repeated film samples of one cured polymer and reported with error bars indicating the minimum and maximum values recorded.

4.3.10 Transmission Electron Microscopy (TEM)

The cured PHU sample was sectioned with a Leica Microsystems EM UC7/FC7 cryo-ultramicrotome (Leica Microsystems, Wetzlar, Germany) with a Diatome diamond knife (Diatome, Nidau, Switerzerland) at -120 °C. The ultrathin sections of ~50 to 70 nm thickness were transferred onto 200-mesh Cu TEM grids with Formvar support film with 2.3 M sucrose in 0.1 M phosphate buffer. The grids containing the sections are washed carefully with distilled water to remove sugar solution and then dried. The grids were then imaged by a Thermo Scientific Talos F200X G2 S/TEM equipped with a X-FEG High Brightness Schottky Field Emission Source and a Ceta 16M 4k x 4k CMOS Camera at an accelerating voltage of 200 keV.

4.3.11 Scanning Electron Microscopy (SEM)

The POSS-containing HPHU sample was sectioned with a Leica Microsystems EM UC7/FC7 cryo-ultramicrotome (Leica Microsystems, Wetzlar, Germany) with a Diatome diamond knife (Diatome, Nidau, Switerzerland) at -120 °C. The ultrathin sections of ~50 to 70 nm thickness were coated with a 4-nm thick of Pt to enhance electrical conductivity and then imaged by the FEI Helios Nanolab 660 DualBeam (FIBSEM) at an accelerating voltage of 2 kV, beam current of 0.40 nA and working distance of 4 mm in secondary electron (SE) mode. Energy dispersive

Spectroscopy (EDS) was performed on the microstructural features to determine elemental composition.

4.3.12 Water Contact Angle Measurements

Water contact angle measurements were performed on an OCA 150 apparatus (DataPhysics Instruments GmbH) with a sessile drop configuration that deposited 5 μL droplet of Milli-Q water at a rate of 0.5 μL s^{-1} with a 0.5 mL GASTIGHT #1750 syringe. SCA20 software was used to determine the mean contact angle from five repeated measurements taken at different points on the sample.

SUPPORTING INFORMATION

Supporting Information is available from the Wiley Online Library or from the author.

ACKNOWLEDGEMENTS

The authors would like to thank the Natural Sciences and Engineering Research Council (NSERC) Collaborative Research and Development grant (CRDPJ 522280-17), the Eugenie Ulmer-Lamothe scholarship (EUL), the Fonds de Recherche du Québec and to the ADFAST Corporation for the funding for this project. The authors would also like to thank the McGill Chemistry Material Characterization facility for assistance and use of their facility. The operation of MC2 and their staff is supported by the Quebec Center for Advanced Materials (QCAM). They would also like to acknowledge the help from Dr. Robin Stein for running their NMR samples throughout the pandemic as well as Weawkamol Leelapornpisit and David Liu of the McGill Faculty for Electron Microscopy Research for help in microscope operation and data collection.

Received: ((will be filled in by the editorial staff))
Revised: ((will be filled in by the editorial staff))
Published online: ((will be filled in by the editorial staff))

CONFLICT OF INTEREST

The authors declare no conflict of interest.

DATA AVAILABILITY STATEMENT

The data that support the findings of this study are available from the corresponding author upon reasonable request.

TABLE OF CONTENTS

ToC Text: Polyhedral oligomeric silsesquioxane (POSS) are added to PHU prepolymers to create HPHUs with enhanced mechanical and thermal properties. These hybrid materials were then further functionalized with 3-Isocyanatopropyl(trimethoxy) silane (IPTMS) via the pendant hydroxyl bonds within the backbone of the polymers to obtain a final cured film comparable to conventional PUs.

ToC Figure:

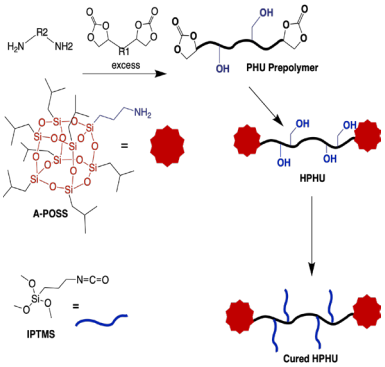

REFERENCES

[1] H. W. Engels, H. G. Pirkl, R. Albers, R. W. Albach, J. Krause, A. Hoffmann, H. Casselmann, J. Dormish, *Angew Chem Int Ed Engl* **2013**, *52*, 9422.

[2] P. Europe, "Plastics - the Facts 2021: An analysis of European plastics production, demand and waste data", A.o.P. Manufacturers, Ed., Brussels - Belgium, 2021https://plasticseurope.org/knowledge.

[3] O. Kreye, H. Mutlu, M. A. R. Meier, *Green Chemistry* **2013**, *15*.

[4] J. Guan, Y. Song, Y. Lin, X. Yin, M. Zuo, Y. Zhao, X. Tao, Q. Zheng, *Industrial & Engineering Chemistry Research* **2011**, *50*, 6517.

[5] United States of America. US2802022 (1957), inv. D. Stephen J. Groszos, and Erhart K. Drechsel;

[6] M. Ghasemlou, F. Daver, E. P. Ivanova, B. Adhikari, *European Polymer Journal* **2019**, *118*, 668.

[7] A. Cornille, S. Dworakowska, D. Bogdal, B. Boutevin, S. Caillol, *European Polymer Journal* **2015**, *66*, 129.

[8] J. H. Clements, *Ind. Eng. Chem. Res.* **2003**, *42*, 663.

[9] T. F. G. Chaoqun Zhang, Samy A. Madbouly, Michael R. Kessler, *Progress in Polymer Science* **2017**, *71*, 91.

[10] S. S. B. Tamami, G. L. Wilkes, *Journal of Applied Polymer Science* **2004**, *92*, 883.

[11] K. Błażek, J. Datta, *Critical Reviews in Environmental Science and Technology* **2019**, *49*, 173.

[12] M. M. Mazurek-Budzyńska, G. Rokicki, M. Drzewicz, P. A. Guńka, J. Zachara, *European Polymer Journal* **2016**, *84*, 799.

[13] K. M. F. Rossi de Aguiar, V. S. Alves, P.-L. M. Noeske, K. Rischka, M. B. Portela, A. Ferreira-Pereira, U. P. Rodrigues-Filho, "Chapter 4 - Hybrid films based on nonisocyanate polyurethanes with antimicrobial activity", in *Materials for Biomedical Engineering*, A.-M. Holban and A.M. Grumezescu, Eds., Elsevier, 2019, p. 77.

[14] H. Asemani, F. Zareanshahraki, V. Mannari, *Journal of Applied Polymer Science* **2019**, *136*, 47266.

[15] J. Ke, X. Li, F. Wang, M. Kang, Y. Feng, Y. Zhao, J. Wang, *Journal of CO2 Utilization* **2016**, *16*, 474.

[16] A. Cornille, J. Serres, G. Michaud, F. Simon, S. Fouquay, B. Boutevin, S. Caillol, *European Polymer Journal* **2016**, *75*, 175.

[17] C. Zhang, H. Wang, Q. Zhou, *Green Chemistry* **2020**, *22*, 1329.

[18] C. Carré, H. Zoccheddu, S. Delalande, P. Pichon, L. Avérous, *European Polymer Journal* **2016**, *84*, 759.

[19] United States of America. US7232877B2 (2002), Homecom Communications Inc, inv. O. Figovsky;

[20] United States of America. US6120905A (1999), Eurotech Ltd, inv. O. L. Figovsky;

[21] United State of America US9102829B2 (2011), Lifschitz Yakov Mark Nanotech Industries Inc, inv. O. F. Olga Birukov, Alexander Leykin, Raisa Potashnikov, Leonid Shapovalov;

[22] T. Bürgel, M. Fedtke, *Polymer Bulletin* **1993**, *30*, 61.

[23] T. Bürgel, M. Fedtke, M. Franzke, *Polymer Bulletin* **1993**, *30*, 155.

[24] G. Rokicki, M. Lewandowski, *Die Angewandte Makromolekulare Chemie* **1987**, *148*, 53.

[25] R. H. Lambeth, A. Rizvi, *Polymer* **2019**, *183*, 121881.

[26] O. Figovsky, L. Shapovalov, O. Birukova, A. Leykin, *Polymer Science Series D* **2013**, *6*, 271.

[27] O. Figovsky, O. Birukov, L. Shapovalov, A. Leykin, *Scientific Israel–Technological Advantages* **2011**, *13*, 122.

[28] K. Wazarkar, M. Kathalewar, A. Sabnis, *European Polymer Journal* **2016**, *84*, 812.

[29] Y. Ecochard, J. Leroux, B. Boutevin, R. Auvergne, S. Caillol, *European Polymer Journal* **2019**, *120*, 109280.

[30] X. Chen, L. Li, T. Wei, D. C. Venerus, J. M. Torkelson, *ACS Appl Mater Interfaces* **2019**, *11*, 2398.

[31] H. Blattmann, R. Mülhaupt, *Macromolecules* **2016**, *49*, 742.

[32] G. Liu, G. Wu, J. Chen, S. Huo, C. Jin, Z. Kong, *Polymer Degradation and Stability* **2015**, *121*, 247.

[33] G. Liu, G. Wu, J. Chen, Z. Kong, *Progress in Organic Coatings* **2016**, *101*, 461.

[34] B. Zhao, K. Wei, L. Wang, S. Zheng, *Macromolecules* **2020**, *53*, 434.

[35] A. K. Nanda, D. A. Wicks, S. A. Madbouly, J. U. Otaigbe, *Macromolecules* **2006**, *39*, 7037.

[36] G. R. Younes, G. Price, Y. Dandurand, M. Maric, *ACS Omega* **2020**, *5*, 30657.

[37] L.-P. Bowman, G. R. Younes, M. Marić, *Macromolecular Reaction Engineering*, *n/a*, 2100055.

[38] G. R. Younes, M. Maric, *Macromolecular Materials and Engineering* **2021**, *306*, 2000715.

[39] G. R. Younes, M. Maric, *Industrial & Engineering Chemistry Research* **2021**, *60*, 8159.

[40] A. Cornille, Y. Ecochard, M. Blain, B. Boutevin, S. Caillol, *European Polymer Journal* **2017**, *96*, 370.

[41] J.-Z. Hwang, S.-C. Wang, P.-C. Chen, C.-Y. Huang, J.-T. Yeh, K.-N. Chen, *Journal of Polymer Research* **2012**, *19*, 9900.

[42] F. Zareanshahraki, H. R. Asemani, J. Skuza, V. Mannari, *Progress in Organic Coatings* **2020**, *138*, 105394.

[43] F. Zareanshahraki, V. Mannari, *Journal of Coatings Technology and Research* **2021**, *18*, 695.

[44] M. Decostanzi, C. Bonneaud, S. Caillol, *Journal of Polymer Science Part A: Polymer Chemistry* **2019**, *57*, 1224.

[45] H. Buchheit, B. Bruchmann, K. Stoll, R. Mülhaupt, *Journal of Polymer Science* **2021**, *59*, 882.

[46] V. Schimpf, A. Asmacher, A. Fuchs, B. Bruchmann, R. Mülhaupt, *Macromolecules* **2019**, *52*, 3288.

[47] G. R. Younes, M. Maric, *Journal of Applied Polymer Science* **2022**, *139*, 52044.

[48] F. Camara, S. Caillol, B. Boutevin, *European Polymer Journal* **2014**, *61*, 133.

[49] R. Villa, R. Porcar, S. Nieto, A. Donaire, E. Garcia-Verdugo, S. V. Luis, P. Lozano, *Green Chemistry* **2021**, *23*, 4191.

[50] S. Jana, H. Yu, A. Parthiban, C. L. L. Chai, *Journal of Polymer Science Part A: Polymer Chemistry* **2010**, *48*, 1622.

[51] B. Ochiai, Y. Ootani, T. Maruyama, T. Endo, *Journal of Polymer Science Part A: Polymer Chemistry* **2007**, *45*, 5781.

[52] R. Morales-Cerrada, B. Boutevin, S. Caillol, *Progress in Organic Coatings* **2021**, *151*, 106078.

[53] E. Rix, E. Grau, G. Chollet, H. Cramail, *European Polymer Journal* **2016**, *84*, 863.

[54] B. Bizet, E. Grau, H. Cramail, J. M. Asua, *ACS Applied Polymer Materials* **2020**, *2*, 4016.

[55] B. Bizet, E. Grau, H. Cramail, J. M. Asua, *European Polymer Journal* **2021**, *146*, 110254.

[56] B. Bizet, É. Grau, H. Cramail, J. M. Asua, *Polymer Chemistry* **2020**, *11*, 3786.

[57] A. Gomez-Lopez, F. Elizalde, I. Calvo, H. Sardon, *Chemical Communications* **2021**, *57*, 12254.

[58] A. Gomez-Lopez, S. Panchireddy, B. Grignard, I. Calvo, C. Jerome, C. Detrembleur, H. Sardon, *ACS Sustainable Chemistry & Engineering* **2021**, *9*, 9541.

[59] A. Bossion, R. H. Aguirresarobe, L. Irusta, D. Taton, H. Cramail, E. Grau, D. Mecerreyes, C. Su, G. Liu, A. J. Müller, H. Sardon, *Macromolecules* **2018**, *51*, 5556.

[60] F. Uhlig, H. C. Marsmann, *Gelest Catalog* **2008**, 208.

[61] S. A. Mirmohammadi, M. Imani, H. Uyama, M. Atai, M. B. Teimouri, N. Bahri-Lale, *Polymer International* **2014**, *63*, 479.

[62] M. Y. L. Chew, *Building and Environment* **2001**, *36*, 925.

[63] N. Ahmed, H. Fan, P. Dubois, X. Zhang, S. Fahad, T. Aziz, J. Wan, *Journal of Materials Chemistry A* **2019**, *7*, 21577.

[64] M. Sánchez-Soto, D. A. Schiraldi, S. Illescas, *European Polymer Journal* **2009**, *45*, 341.

[65] K. L. Frank, S. E. Exley, T. L. Thornell, S. E. Morgan, J. S. Wiggins, *Polymer* **2012**, *53*, 4643.

[66] A. Feinle, F. Leichtfried, S. Straßer, N. Hüsing, *Journal of Sol-Gel Science and Technology* **2017**, *81*, 138.